International Journal of Engineering, Science and Information Technology
Volume 5, No. 4 (2025) pp. 28-36
eISSN: 2775-2674
Website: http://ijesty.org/index.php/ijesty
DOI: https://doi.org/10.52088/ijesty.v5i4.1196
Research Paper, Short Communication, Review, Technical Paper

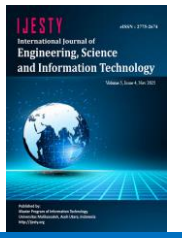

Artificial Intelligence Driven Skin Cancer Detection Using R-FCN Enhanced Deep Convolutional Neural Networks with SMOTE Balancing

A Ronald Doni[1]*, Chin-Shiuh Shieh[2], Siva Shankar S[3], Prasun Chakrabarti[4], G Nagarajan[5], S Murugan[5]

[1]National Kaohsiung University of Science and Technology, Taiwan
[2]Department of Electronics Engineering, National Kaohsiung University of Science and Technology, Taiwan
[3]Department of Computer Science and Engineering, Sir Padampat Singhania University, Rajasthan, lndia
[4]Department of CSE, KG Reddy College of Engineering and Technology, Hyderabad, Telangana, India
[5]Department of Computer Science and Engineering, Sathyabama Institute of Science and Technology, Chennai, India

**Corresponding author E-mail: ronaldtony.a@gmail.com*

The manuscript was received on 15 February 2025, revised on 22 April 2025, and accepted on 12 August 2025, date of publication 2 November 2025

Abstract

Skin cancer is a serious worldwide health issue, and earlier diagnosis is crucial for patient outcomes and efficient treatment. However, due to the variety of skin cancer types and the complexity of medical imaging, making an accurate diagnosis can be challenging. This study tackles this issue by introducing a new deep learning (DL) algorithm that is specifically designed for skin tumor diagnosis and employs the Convolutional Neural Network (CNN) technology. This study offers a novel approach that makes use of Region-based Fully Convolutional Networks (R-FCN) to address the crucial problem of skin cancer lesion categorization. The suggested system seeks to increase classification efficiency by using region-based detection which improves classification accuracy and localization. The HAM10000 and ISIC-2020 datasets, which are difficult and unbalanced, were used to thoroughly evaluate the created Deep CNN (DCNN) architecture. The Synthetic Minority Over-sampling Technique (SMOTE) was purposefully used as the method of random sampling in order to lessen the imbalanced datasets. This greatly enhanced the suggested models generalization and robustness. The results demonstrate the remarkable efficacy of the research contribution, yielding performance metrics consistently above 98% for F1-score, specificity, sensitivity, recall, accuracy, precision, and the area under the ROC curve (AUC). In terms of balancing speed and accuracy the suggested approach also performs better than traditional methods like R-CNN and YOLOv8. The study demonstrates that a strong framework for automatic skin cancer detection and classification is provided by combining R-FCN with SMOTE and CNN techniques. This framework facilitates early diagnosis and aids dermatologists in clinical decision-making.

Keywords: *Convolutional Neural Network, R-FCN, Deep CNN, Synthetic Minority Over-sampling Technique, Artificial Intelligence.*

1. Introduction

The skin serves as a protective barrier against various injuries and diseases, preventing moisture loss and absorbing UV radiation due to the pigment melanin. The skin is composed of three layers: the surface layer, or epidermis; the middle layer, or dermis, which includes sweat glands and connective tissue; and the layer underneath, or the dermis,, which is primarily made up of fat [1]. Skin cancer is most widespread types of cancer, and if caught early enough, the prognosis is favorable [10]. Skin cancer is highly dangerous due to its rapid spread, but early detection can significantly reduce risks and improve treatment outcomes. When DNA damage causes normal skin cells to turn malignant, resulting in unchecked cell proliferation and aberrant cell morphologies, skin cancer occurs. According to histology, the skin cancer cells have irregular shapes and differentiate in its cytoplasm, nucleus, and nucleosome [6]. Basal-cell carcinoma (BCC), squamous-cell carcinoma (SCC), and melanoma, are the three different classification of Skin cancers arise from irregular cell production with the latter being the most dangerous. Symptoms of the melanoma include changes in moles, such as changes in scale, form, color, and border irregularity. Globally, 287,723 new melanoma cases were recorded in 2018, leading to 60,712 deaths. In the US alone, nearly 96,480 cases were reported in 2019, resulting in about 7,230 deaths. Ultraviolet radiation exposure is a key environmental factor contributing to skin cancer. Early diagnosis of melanoma significantly increases survival rates, highlighting the importance of research into its detection and classification. Traditional methods like biopsies are invasive and time-consuming, for automated skin cancer

detection the leading researchers are currently exploring the artificial intelligence (AI) and deep learning (DL) methods in a comprehensive way [25]. Artificial Neural Networks (ANN) and Convolutional Neural Networks (CNN), two machine learning (ML) techniques, have demonstrated encouraging outcomes in correctly recognizing melanoma and non-melanoma lesions [24]. CNNs have transformed the diagnosing the skin cancer by accurately classifying lesions through feature extraction. The study highlights that CNN is more effective than ANN for skin cancer detection due to its superior image classification capabilities. It emphasizes the need for an automated AI-based system to improve diagnostic accuracy, reduce detection time, and assist dermatologists in making early, accurate diagnoses. Future improvements should address dataset limitations and refine AI models for broader applicability. Neural networks require extensive training, high computational power, and large, diverse datasets. Variability in lesion size, imbalanced datasets, and limited image diversity (age, skin tone) present classification challenges. CNN specializes in image processing using convolution, pooling, and fully connected layers for extracting and classifying the sample data features [26]. Several CNN-based models achieved accuracy above 90%, demonstrating their potential for skin cancer detection. Advanced CNN models integrate additional techniques like data augmentation, transfer learning, and region-based CNN (R-CNN) to enhance classification accuracy.

2. Literature Review

2.1. Skin Cancer

In order to predict non-melanoma skin tumor, [1] created a multi-parameterized ANN architecture using individual health data. It examined thirteen personal health parameters and obtained good sensitivity and specificity. The model trained on the PH2 dataset (200 pictures) was implemented by [2], achieving 97.7% accuracy in identifying skin lesions that are benign or cancerous. Using first-order feature extraction techniques and an ANN-based multilayer perceptron model, [7] increased the classification accuracy of melanoma detection. Nevus pigmentosus is a benign cancer that develops from melanocytes, which are dendritic cells that generate pigment between keratinocytes in the basal layer of the epidermis), can be dangerous and difficult to manage. Characterized by birthmarks or moles can develop into deadly melanoma when early detection is not done and these problems arises when the skin is exposed to pollution, UV light, and other harmful chemicals. Patients with complications may also suffer from neurological disorders, including seizures, fainting, and vomiting [14]. One hazardous form of skin cancer that starts in the skin is melanoma and can start spreading into the other parts of the body. Originating from melanocytes (melanin-producing cells in the skin) are irregular in shape with multiple colors. Affected moles may be itchy, bleed, and are often larger than normal moles [15].

2.2. CNN

[5] Explored CNN's ability to classify skin lesions using patient data and lesion images, achieving improved accuracy when combining both features. Utilizing the ISIC (International Skin Imaging Collaboration) database for training, [6] built a CNN-based classification of skin tumor, and the generated model attains 97.49% of accuracy. The study used a CNN to create an automated approach for classifying benign tumor lesions and skin cancer. Three hidden layers with channel capacities of 16, 32, and 64 make up the suggested model. The Adam optimizer outperformed the other optimizers examined, obtaining a 99% accuracy level in recognizing cutaneous lesions from the ISIC sample. Squamous cell carcinoma, nevus pigmentosus, dermatofibroma, and melanoma are the four classes into which the classification is divided. A comprehensive study of CNN usage for skin lesion categorization was conducted by [3], finding that CNN outperformed dermatologists in melanoma detection when trained on large datasets. [4] Integrated CNN with Natural Language Processing (NLP) in a chatbot-based skin cancer detection application, achieving 99.35% accuracy. [7] applied Region-Based CNN (R-CNN) for automatic lesion segmentation and classification, leading to a diagnostic accuracy comparable to dermatologists. [7] Combined CNN with Whale Optimization Algorithm (WOA) to fine-tune weights and improve melanoma detection. In this study, the authors developed a R-CNN which formulates the images into region based and are applied for detecting the keratinocytic skin cancer on facial images. Dataset which comprises of clinical images is the input (training, testing and validating) for the algorithm and results in high performance for recognizing skin tumor lesions and the work also highlighs the potential of DL models in dermatological diagnostics. [8] Applied the CNN algorithm with incremental data techniques for overcoming the issue of limited training data and achieving significant improvements in classification accuracy. [9] Implemented a parallel CNN architecture for nine different skin tumor types, improving overall classification accuracy to 79.45%.

[2] formulate the methods that can classifies the whether the cells belongs to both benign and malignant skin lesions, but the technique might be improved in terms of precision and the suggested approach that combines a Maximum Gradient Intensity (MGI) algorithm for hair pixel detection, different categories of shape and several texture features, and the classifier of type artificial neural network. An efficient method for separating benign and malignant skin tumors is produced by combining the computer science fields of AI and image processing. Many methods for automatically detecting melanoma have been created by scientists and researchers, which makes therapy less subjective and reduces complications. For instance, [11] proposed a digital diagnostic technique for early melanoma identification, ABCD rule is combined with region-growing segmentation [12]. Computer-assisted melanoma detection systems acquire dermoscopic images, remove noise, segment using Maximum Entropy Thresholding, collect features with Gray Level Co-occurrence Matrix (GLCM), and classify using ANN [13].

A CNN-based method was created by [6] to automatically recognize benign tumor lesions and skin tumor. Using the Adam optimizer (with a 0.001 learning rate) on the ISIC dataset, their CNN model with three hidden layers classified lesions into four kinds with 99% accuracy. [16] Investigated the usage of raw images, DL, and few-shot learning for skin lesion analysis, specifically examining the impact of CNNs on texture analysis. The authors also have addressed the challenge of class imbalance through techniques like transfer learning, data augmentation, GANs, various sampling methods, and different loss functions. This study is compared with the ensemble and hybrid models for early detection and the advancements and ongoing difficulties in this domain of research. The authors explained the classification enables learning from limited labeled data, while DL, particularly CNNs, extracts crucial features from images for skin cancer diagnosis, overcoming limitations faced by traditional ML. CNNs have a structure where each node connects to a limited amount of nodes in the next layer [17].

The following survey employs ANN with Backpropagation for skin lesion classification using different datasets and feature extraction techniques. The study [18] classifies melanoma by considering thirty one dermoscopic images and extracts the features with a 96.9% accuracy rate based on the parameters of Asymmetry, Border irregularity, Color variation, and Diameter (ABCD). Using 90 dermoscopic pictures, [19] apply maximum entropy for thresholding technique and GLCM for texture-based feature extraction to differentiate melanoma from nonmelanoma with an accuracy of 86.6%. Using 31 dermoscopic pictures, the authors [20] distinguish between malignant and noncancerous lesions by applying thresholding for segmentation and 2D wavelet transform analysis for extracting the

features. The varying accuracy levels reflect the effectiveness of different feature extraction techniques, with the ABCD parameters yielding the highest accuracy, while texture-based and wavelet-based approaches show competitive but slightly lower performance.
[22] Introduced an innovative DCNN for the classification of skin tumor, evaluated on two datasets which are unbalanced in nature, ISIC-2019 and HAM10000. Transfer learning models such as VGG16, VGG-19, DenseNet-121, DenseNet-201, and MobileNet-V2 are contrasted with the DCNN model. The metrics accuracy, recall, precision, F1-score, specificity, and AUC are employed to evaluate these methods. The results of the experiment show that the suggested DCNN performs better than the different DL models tested, achieving **98.5% accuracy on HAM10000** and **97.1% on ISIC-2019**, demonstrating its effectiveness in handling class imbalance and improving classification accuracy. Additionally, it surpasses other research outputs using the similar datasets, highlighting its robustness and superior performance in skin cancer detection.

2.3. Dataset

1. HAM10000:
   A range of skin tumor photos are included in the datasets, and DL techniques typically requires a huge volume of data for achieving desirable and accurate results. However, collecting a diverse set of skin cancer images is challenging, and limited availability of training data poses a significant obstacle for DL applications. To overcome these challenges, 10,000 trained images from the Human Against Machine (HAM10000) dataset were used, along with 10,015 dermoscopic images. These pictures show skin lesions that fall into seven different categories: Actinic keratoses (ak-327 images), basal cell carcinoma (bcc-514 images), dermatofibroma (d-115 images), melanoma (m-1113 images), vascular lesions (v-142 images), melanocytic nevi (mn-6705 images), and benign keratosis-like lesions (bk-1099 images). The HAM10000 collection is widely used in dermatological research to conduct tests pertaining to the classification of skin tumors, as it encompasses the broad spectrum of various conditions of the skin observed in the clinical settings, this makes the HAM10000 is valuable resource for evaluating the image classification on dermatoscopic image. However, there is a class imbalance in the dataset, with notably fewer samples in certain categories than in others.

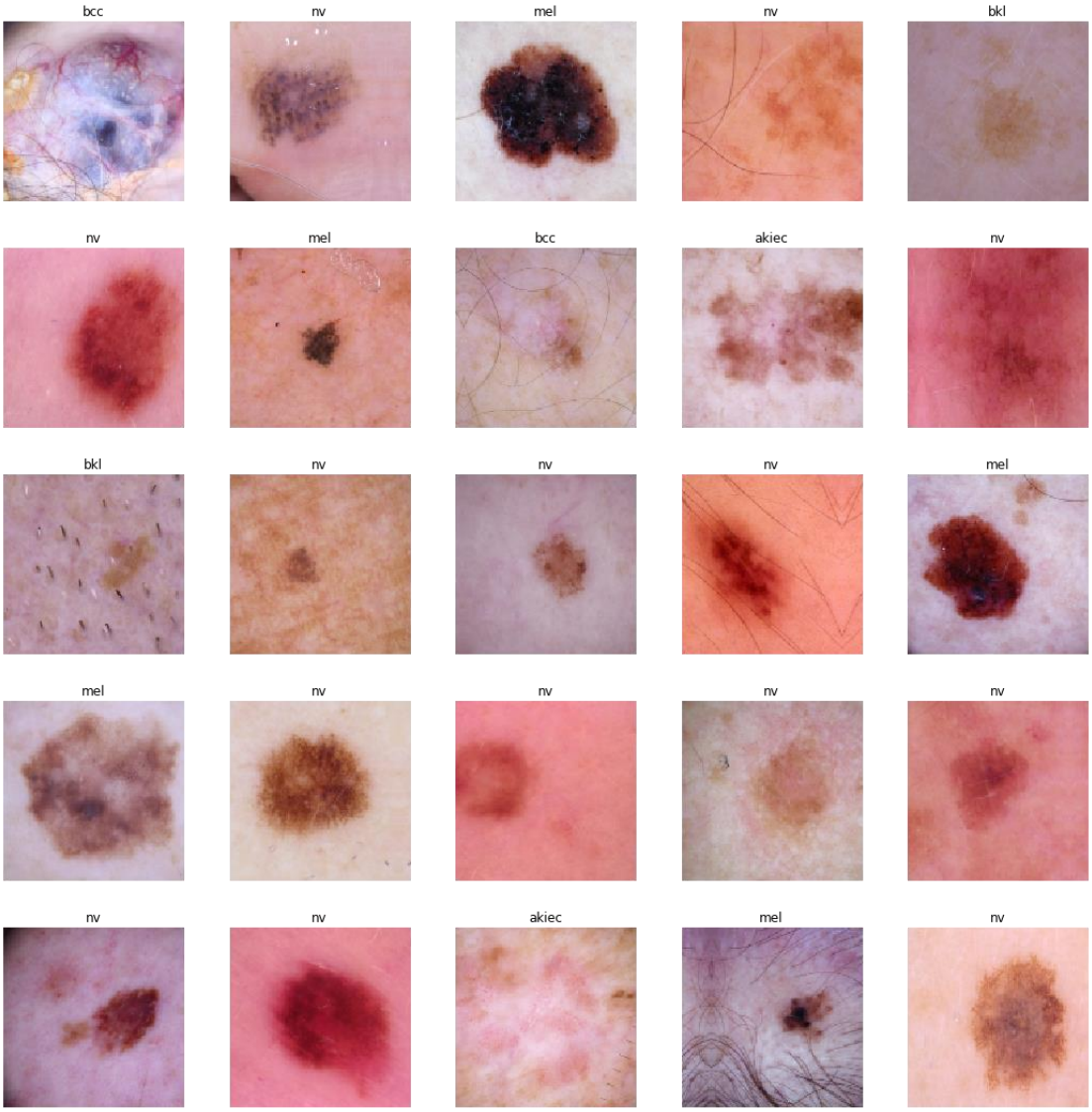

Fig 1. HAM10000 Dataset (github) [23]

2. ISIC-2019:
   Dermoscopic photos from the International Skin Imagining Collaboration (ISIC) are included in the ISIC-2020 collection. These images are intended to be used for the general classification of skin tumors into nine distinct diagnostic types. The main goal of this dataset is to create ML models that can automatically recognize skin lesions based on visual characteristics. 10,982 testing and 33,126 training images in DICOM make up the ISIC dataset and JPEG templates along with metadata, grouped separated into eight

training courses, each of which is related to the distinct clinical label that denotes the classes of skin lesion. One of the biggest publicly accessible datasets for classifying skin lesions is ISIC; ISIC-2020 includes a wide variety of skin disorders, serving as a complete benchmark for evaluating dermatoscopic image analysis when used on various algorithms. Figure 2, shows the images of ISIC-2019 dataset [21].

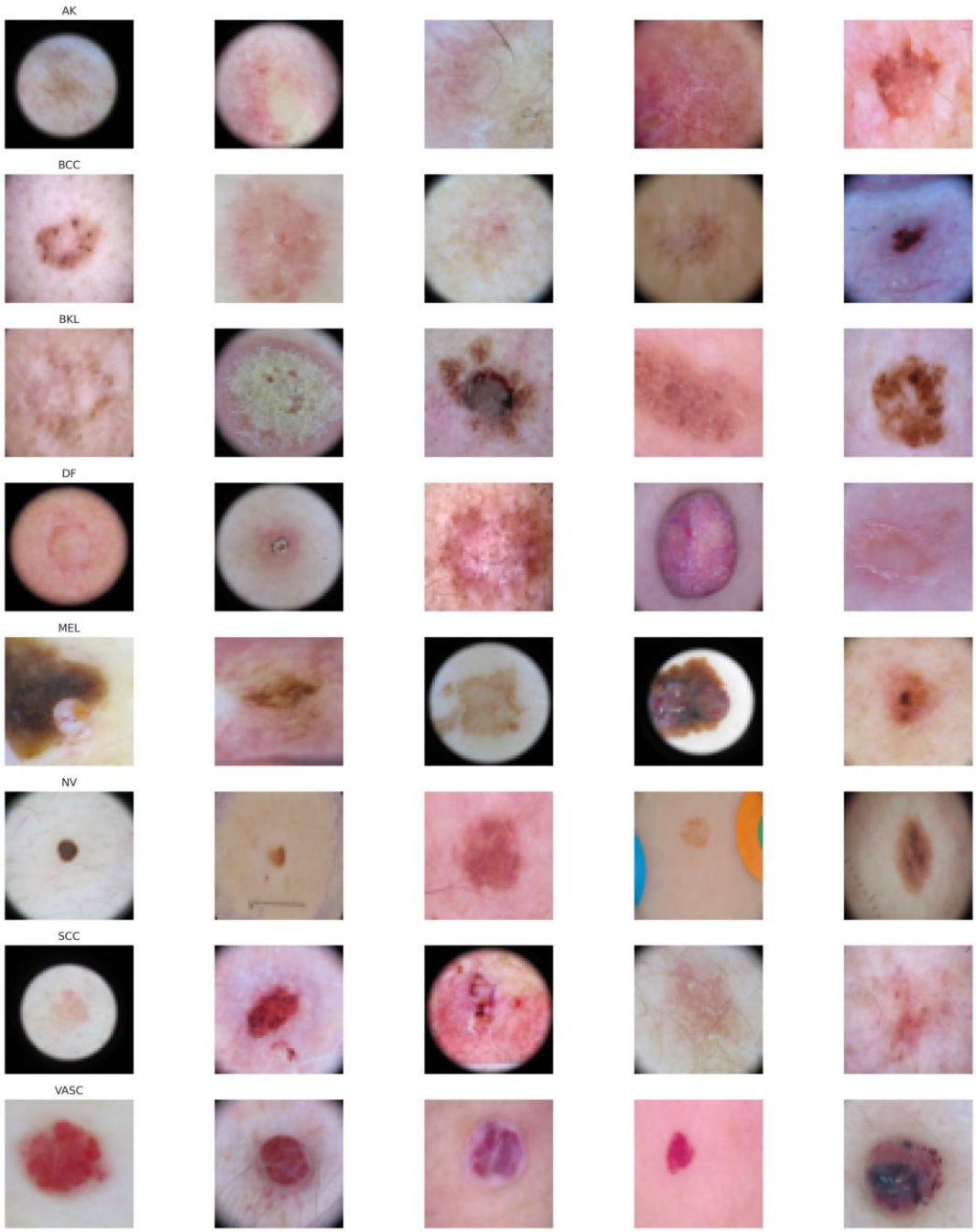

Fig 2. ISIC-2019 Dataset

To reduce the disparity in classes in the information sets, the SMOTE is used HAM10000 and ISIC-2020. The SMOTE technique providing the guarantee that the proposed R-FCN model is trained with a more balanced distribution of classes, fostering equitable learning and improving generalization across various categories. Implementing SMOTE approach enhances model robustness and improves the performance on various measures in the classication of dermatoscopic images. Instead of simply duplicating available classes using the minority class samples, the SMOTE approach generates the samples which are synthetic in nature and is achieved by calculating the interpolation the known data points. The methodology assists in reducing the overfitting and improves the generalization.

3. Methods

In general, the Region of Interest (ROI) is divided into a section of 3 × 3 and the ROI pool with 3× 3. In the proposed model, the ROI pool generalizes them into k× k that is the number of score maps required is k × k × (C+1). Therefore, the proposed R-FCN based approach considers the feature maps and apply the convolution by creating the score maps which are position centric and with the depth level being k × k × (C+1). In every region of interest, position-sensitive ROI pool is applied for generating the vote array with the

dimension shape of k × k. The average of the array data is considered in the classifying phase and is achieved by evaluating them using the softmax approach. The working procedure is given in Figure 3.

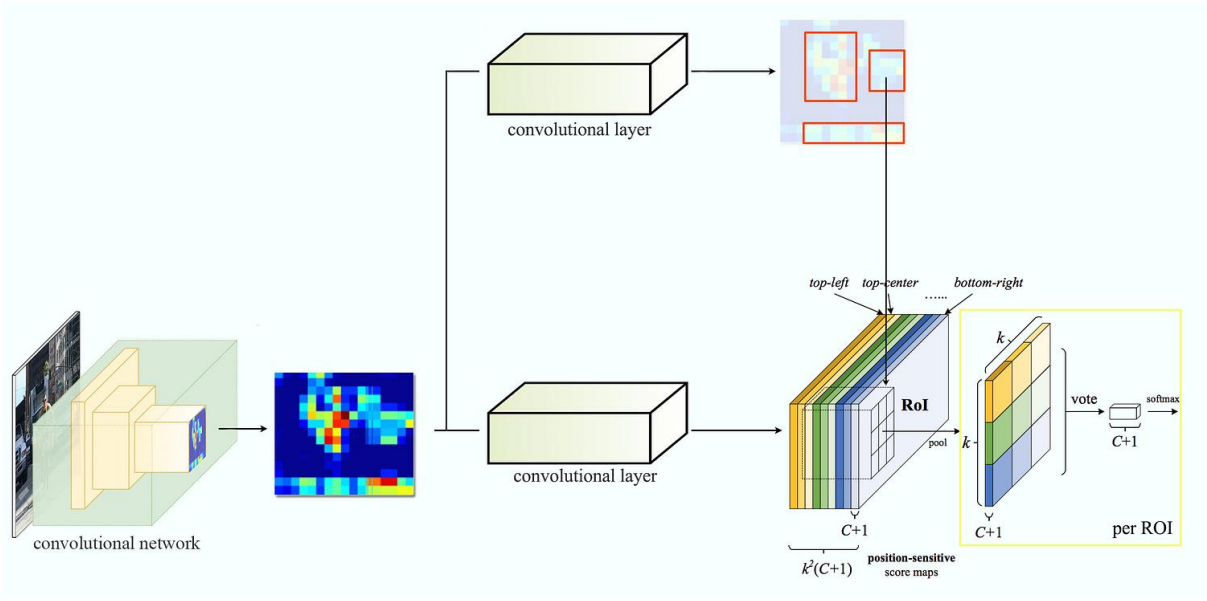

Fig 3. R-FCN Network Flow

Description of the process:

1. **Input Image & Convolutional Feature Extraction**:
   The left-most section of the image shows an input image being processed by a **CNN**. This CNN extracts **feature maps**, which encode spatial and semantic information about objects in the image. The convolutional network results in a **heatmap-like representation** of the image, where regions of high activation likely correspond to object locations.
2. **Convolutional Layers for Feature Extraction:**
   The extracted feature map is then fed into additional **convolutional layers** (as indicated by two large convolutional layer blocks). These layers refine and learn more complex feature hierarchies to improve localization and classification accuracy.
3. **Region of Interest (RoI) Pooling & Position-Sensitive Score Maps:**
   The concept of **position-sensitive score maps** is the subsequent section of the proposed model. Unlike standard **RoI Pooling** (which are applied in Faster R-CNN), R-FCN applies tge **position-sensitive RoI pooling** in order to retain the spatial information. The feature map is divided into **k × k bins** for each RoI, where each bin represents the precise part of an object.
4. **Classification and Bounding Box Regression**:
   The right-most section in the architecture highlights the classification process. The extracted RoI features are used to **vote** for the object class. A **softmax function** is applied over the pooled features to produce final classification scores. The model predicts **(C+1)** scores per RoI, in which C represents the amount of object classes, and "+1" accounts for the background class.

3.1. Mathematical Representation of the Model

3.1.1. Convolutional Feature Extraction

Given an input image with dimensions H×W×3, a CNN extracts feature maps F:

$$I \in \mathbb{R}^{H \times W \times 3} \tag{1}$$

In the equation, H and W are the image height and width, and 3 represents RGB color channels.
F=fconv(I)
Where, fconv represents the function learned by the convolutional network.
Let F have dimensions H′×W′×D, and D indicates the number of channels.

3.1.2. RoI Extraction and Position-Sensitive Score Maps

Instead of directly using RoI pooling, R-FCN constructs **position-sensitive score maps**.
If there are C object classes, we generate $k^2(C+1)$ score maps:
S=fconv2(F)
Where, S has dimensions $H' \times W' \times k^2(C+1)$.
For each RoI, we divide it into k×k bins and map each bin to the corresponding **position-sensitive score maps**. Let an RoI be defined by coordinates (x_1,y_1,x_2,y_2), and let each bin be indexed by (i,j), where (x_1,y_1) and (x_2,y_2) are the **top-left** and the **bottom-right** corner of the region. The pooled value for a specific bin is:

$$P_{i,j} = \frac{1}{|R_{i,j}|} \sum_{(x,y) \in R_{i,j}} S_{i,j}(x,y) \tag{2}$$

where:

1. $R_{i,j}$ refers to the set of pixels in the $(i,j)^{th}$ bin.
2. $S_{i,j}$ represents position-sensitive score maps.

The final **class score for RoI** is obtained by summing over all bins:

$$s_c = \sum_{i,j} P_{i,j} \tag{3}$$

where s_c is the score for class c

3.1.3. Classification Using Softmax

Once the pooled features are obtained, then the **softmax function** is employed in order to obtain the final probabilities:

$$s_c = \sum_{i,j} P_{i,j} \tag{4}$$

where p_c is the probability of RoI that belongs to the class c.

3.1.4. Bounding Box Regression

The model also predicts bounding box offsets for each RoI using regression:

$$(\Delta x, \Delta y, \Delta w, \Delta h) = f_{\text{reg}}(P) \tag{5}$$

where:

1. (Δx,Δy) are the predicted center offsets.
2. Δw,Δh) are the width and height adjustments.

The required bounding box coordinates are given by:

$$\hat{x} = x + w \cdot \Delta x, \quad \hat{y} = y + h \cdot \Delta y$$
$$\hat{w} = w \cdot e^{\Delta w}, \quad \hat{h} = h \cdot e^{\Delta h} \tag{6}$$

Summary:

Step	Mathematical Expression
Feature Extraction	$F = f_{\text{conv}}(I)$
Score Map Generation	$S = f_{\text{conv2}}(F)$
Position-Sensitive RoI Pooling	(P_{i,j} = \frac{1}{
Class Score Computation	$s_c = \sum_{i,j} P_{i,j}$
Softmax Classification	$p_c = \frac{e^{s_c}}{\sum_{c'} e^{s_{c'}}}$
Bounding Box Regression	$(\Delta x, \Delta y, \Delta w, \Delta h) = f_{\text{reg}}(P)$
Final Bounding Box Adjustment	$\hat{x} = x + w \cdot \Delta x, \hat{w} = w \cdot e^{\Delta w}$

4. Result and Discussion

Figure 4, shows the sample Melonama image which is given as the input to the proposed model.

Fig 4. Melanoma Image

The intermediate process in which the image flows through is given in Figure 5.

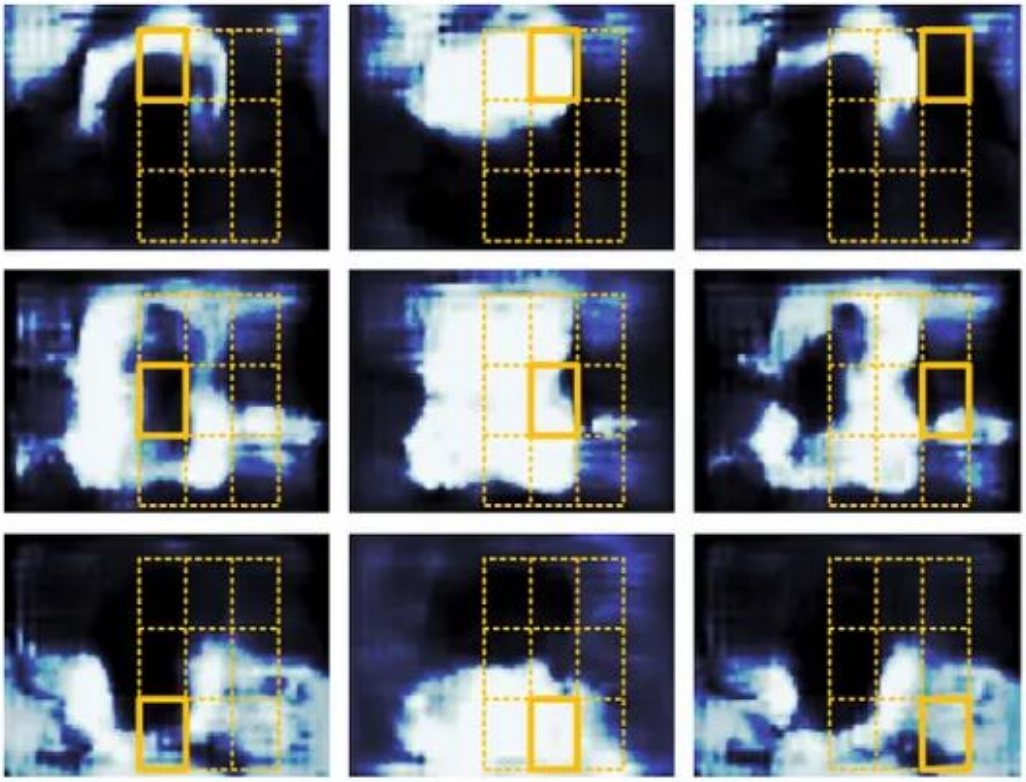

Fig 5. Region of Interest

Figure 6 shows the selection and identification of the image status.

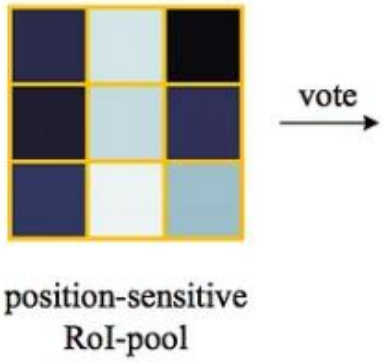

Fig 6. Identification of the Skin Cancer Status (Normal / Cancerous) Cell

Similar type of test is carried out for both the datasets HAM10000 and ICIS-2020 datasets. The proposed model is compared with the existing approaches like R-CNN and YOLO 8. The comparison parameters are demonstrated in Table 1.

Table 1. Comparison R-CNN, YOLO 8 and R-FCN Models for detecting Skin Cancer

Model	Type	Key Idea	Speed	Accuracy	Speed (FPS)	Accuracy (mAP)
R-CNN	Two-stage	Extracts region proposals, runs CNN for each region	Slow (Very High Computation)	High	0.02 FPS (47 sec/img)	High (≈ 60%)
R-FCN	Two-stage	Uses RPN + Position-Sensitive RoI Pooling for better efficiency	Faster than R-CNN, Slower than YOLO	High	5-10 FPS	High (≈ 75%)
YOLO	Single-stage	Predicts bounding boxes + class in one pass over the image	Very Fast (Real-time)	Moderate (Lower than R-CNN & R-FCN)	45-60 FPS	Moderate (≈ 50-55%)

4.1. Performance Analysis of R-FCN Model for HAM10000 and ICIS-2020 Datasets

In the first part of the analysis, the selection of samples and their performance is compared. In this work, SMOTE is applied for the purpose of sampling. The comparison between random sampling and SMOTE on various performance is measures is given in the Table 2.

Table 2. Comparison between SMOTE and Random Sampling – HAM10000

Sampling Method	Accuracy	Recall	Precision	F1Score	Specificity	AUC
SMOTE	98.50%	98.62%	98.47%	98.45%	98.99%	99.01%
Random Sampling	92.21%	92.21%	94.29%	93.46%	96.12%	98.29%

Table 3. Comparison between SMOTE and Random Sampling – ICIS-2020

Sampling Method	Accuracy	Recall	Precision	F1Score	Specificity	AUC
SMOTE	98.15%	98.22%	98.27%	98.65%	98.88%	99.12%
Random Sampling	92.87%	92.42%	94.30%	93.34%	95.92%	98.92%

From the Table 3, it is evident that the SMOTE method outrated the random sampling method when used alongside with R-FCN for both HAM10000 and ICIS2020 datasets.

5. Conclusion

An efficient object detection pipeline using R-FCN with position-sensitive RoI pooling. Compared to Faster R-CNN, this approach is more computationally efficient as it avoids redundant computations in the fully connected layers. The mathematical formulation ensures that spatial information is preserved, leading to better localization and classification accuracy. In the current work, the standard datasets HAM10000 and ICIS-2020 is applied on R-CNN, R-FCN and YOLOv8. In the future, the technique is to be compared with the standard development models like VGG16, VGG19, DensNet121, DensNet201, MobileNetV2, DCNN and with other dataset. The datasets HAM10000 and ICIS2020 suffers from data imbalanced issue and this issue is handled effectively using SMOTE approach.

References

[1] D. Roffman, G. Hart, M. Girardi, C. J. Ko, and J. Deng, "Predicting non-melanoma skin cancer via a multi-parameterized artificial neural network," *Scientific Reports,* vol. 8, no. 1, 2018. https://doi.org/10.1038/s41598-018-19907-9.

[2] P. P. Tumpa and M. A. Kabir, "An artificial neural network based detection and classification of melanoma skin cancer using hybrid texture features," *Sensors International*, vol. 2, 2021. https://doi.org/10.1016/j.sintl.2021.100128.

[3] T. J. Brinker et al., "Skin cancer classification using convolutional neural networks: Systematic review," *J. Med. Internet Res.,* vol. 20, no. 10, 2018. https://doi.org/10.2196/11936.

[4] X. Gong and Y. Xiao, "A skin cancer detection interactive application based on CNN and NLP," in *J. Phys.: Conf. Ser.,* vol. 2078, 2021. https://doi.org/10.1088/1742-6596/2078/1/012036.

[5] J. Höhn et al., "Integrating patient data into skin cancer classification using convolutional neural networks: Systematic review," *J. Med. Internet Res*., vol. 23, no. 7, pp. e20708, 2021. https://doi.org/10.2196/20708.

[6] Y. N. Fu'adah, N. K. C. Pratiwi, M. A. Pramudito, and N. Ibrahim, "Convolutional Neural Network (CNN) for Automatic Skin Cancer Classification System," in *IOP Conf. Ser.: Mater. Sci. Eng*., vol. 982, no. 1, p. 012005, 2020. [Online]. Available: https://doi.org/10.1088/1757-899X/982/1/012005.

[7] S. S. Han, I. J. Moon, W. Lim, I. S. Suh, and S. E. Chang, "Keratinocytic Skin Cancer Detection on the Face Using Region-Based Convolutional Neural Network," *JAMA Dermatol*., vol. 155, no. 1, pp. 29–37, 2019. https://doi.org/10.1001/jamadermatol.2018.4004.

[8] T. C. Pham, C. M. Luong, M. Visani, and V. D. Hoang, "Deep CNN and data augmentation for skin lesion classification," in *Lecture Notes in Computer Science*, vol. 10752, Springer, 2018, pp. 573–582. 10.1007/978-3-319-75420-8_54.

[9] N. Rezaoana, M. S. Hossain, and K. Andersson, "Detection and classification of skin cancer by using a parallel CNN model," in *Proc. IEEE Int. Women in Eng. (WIE) Conf. Elect. Comput. Eng*., 2020, pp. 380–386. doi: 10.1109/WIECON-ECE52138.2020.9397987.

[10] A. Shah et al., "A comprehensive study on skin cancer detection using artificial neural network (ANN) and convolutional neural network (CNN)," *Clin. eHealth*, vol. 6, pp. 76–84, 2023. doi: 10.1016/j.ceh.2023.08.002.

[11] N. Smaoui and S. Bessassi, "A developed system for melanoma diagnosis," *Int. J. Comput. Vis. Signal Process*., vol. 3, no. 1, pp. 10–17, 2013.

[12] M. Kruk, B. Swiderski, S. Osowski, J. Kurek, M. Slowinska, and I. Walecka, "Melanoma recognition using extended set of descriptors and classifiers," *EURASIP J. Image Video Process*., vol. 2015, no. 43, 2015.

[13] D. Kokitkar, A. Amberkar, V. Giri, and K. Krishna, "Computerized automated detection of skin cancer," *Int. J. Adv. Res. Comput. Commun. Eng*., vol. 5, pp. 579–581, 2016.

[14] R. D. Tsaniyah, A. Aspitriani, and Fatmawati, "Prevalensi dan Gambaran Histopatologi Nevus Pigmentosus di Bagian Patologi Anatomi Rumah Sakit Dr. Mohammad Hoesin Palembang," *Periode 1* Januari 2009–31 Desember 2013.

[15] M. Rastrelli, S. Tropea, C. R. Rossi, and M. Alaibac, "Melanoma: Epidemiology, risk factors, pathogenesis, diagnosis and classification," *In Vivo*, vol. 28, no. 6, pp. 1005–1011, Nov–Dec. 2014.

[16] O. Akinrinade and C. Du, "Skin cancer detection using deep machine learning techniques," *Intell.-Based Med*., vol. 11, p. 100191, 2025. doi: 10.1016/j.ibmed.2024.100191.

[17] P. Sabouri and H. GholamHosseini, "Lesion border detection using deep learning," in *Proc. Congr. Evol. Comput. (CEC)*, Vancouver, BC, Canada, Jul. 2016.

[18] T. Kanimozhi and D. A. Murthi, "Computer-aided melanoma skin cancer detection using artificial neural network classifier," *J. Sel. Areas Microelectron*., vol. 8, pp. 35–42, 2016.

[19] R. Aswin, J. Jaleel, and S. Salim, "Artificial neural network based detection of skin cancer," *Int. J. Adv. Res. Elect. Electron. Instrum. Eng.*, vol. 1, pp. 200–205, 2012.

[20] G. Delgado, W. F. Cueva, F. Munoz, and G. Vasquez, "Detection of skin cancer 'melanoma' through computer vision," in *Proc. IEEE Int. Conf. Electron., Electr. Eng. Comput. (INTERCON)*, Cusco, Peru, Aug. 2017, pp. 1–4.
[21] E. H. Houssein, D. A. Abdelkareem, G. Hu, M. A. Hameed, I. A. Ibrahim, and M. Younan, "An effective multiclass skin cancer classification approach based on deep convolutional neural network," *Cluster Comput*., vol. 27, pp. 12799–12819, 2024. doi: 10.1007/s10586-024-04540-1.
[22] P. Tschandl, C. Rosendahl, and H. Kittler, "The HAM10000 dataset, a large collection of multi-source dermatoscopic images of common pigmented skin lesions," *Sci. Data*, vol. 5, p. 180161, 2018.
[23] GitHub Repository, "Skin Cancer Detection." [Online]. Available: https://github.com/temcavanagh/Skin-Cancer-Detection [Accessed: Mar. 31, 2025].
[24] V. Rotemberg et al., "A patient-centric dataset of images and metadata for identifying melanomas using clinical context," Sci. Data, vol. 8, p. 34, 2021. doi: 10.1038/s41597-021-00815-z.
[25] S. D. Putra, M. B. Ulum, and D. Aryani, "Expert system for diagnosis of uterine myomas using the certainty factor method," *Int. J. Eng. Sci. Inf. Technol.*, vol. 1, no. 4, pp. 103–108, 2021.
[26] T. P. Handayani and W. Hasyim, "Comparative analysis of CNN-RNN models for hatespeech detection incorporating L2 regularization," *Int. J. Eng., Sci. Inf. Technol.*, vol. 4, no. 1, pp. 39–43, 2024.